Multiphoton process in cavity QED photons for implementing a three-qubit quantum gate operation

Moteb M. Alqahtani[1]

Abstract

Based on cavity QED of free atoms, we theoretically investigate the implementation of a three-qubit quantum phase gate in which the three qubits are represented by the photons in modes of the cavity. A single four-level atom in double-V type passing through the high-Q cavity is used to implement the gate. We apply the theory of multiphoton resonance and use two-level effective Hamiltonians to predict the proper values for detunings, coupling constants, and interaction times. By the use of both the density matrix approach and wave function method, the influence of the decoherence processes is theoretically and numerically analyzed. Further, we address the effects of deviation in detunings and coupling coefficients and find that the gate operation is substantially insensitive to such variations. Finally, we show that the proposed scheme here can be extended for the implementation of multiqubit quantum phase gates.

1 Introduction

Over the last few decades, there has been great interest in quantum computing research, and one of the most important focal points for the research groups in this field is the construction of a quantum computer [1]. The aim in quantum computing is basically to harness both the principle of superposition and coherent entanglement in applications. It has been shown that quantum computing is one of the most promising applications of quantum mechanics to technology [2] and computational power for particular tasks can be dramatically improved by the use of quantum computing [3–5]. For the implementation of quantum computation, a physical system should possess the following main requirements [6]: (i) Efficient manipulation which includes the ability to initialize

✉ Moteb M. Alqahtani
moalqhtani@kku.edu.sa

1   Department of Physics, King Khalid University, P.O.Box 960, Abha, Asir 61421, Saudi Arabia

the state of the qubits and the ability to implement a universal set of quantum gates; (ii) the capability to reliably measure the individual qubit's state; (iii) a physical system works in the strong coupling regime; in other words, the gate operation time is much shorter than qubit decoherence times; and (iv) a physical system should be scalable with well-characterized qubits. Since the initial formulation of these requirements, several physical systems have been invented or developed further for the purpose of quantum computation (see for example [7–13]).

Among physical systems proposed as candidates for quantum computing implementation, physical systems based on cavity QED offer a promising means as they benefit from a long history of their advantage in entanglement generation and coherent manipulation [11,14,15]. Focusing upon cavity QED of free atoms both in microwave and optical domains, in experiments in which Rydberg atoms interact with a microwave cavity QED, it has been demonstrated that the atoms and the cavity can be prepared in pure states, the strong coupling conditions are readily fulfilled, atoms can be efficiently detected by state-selective detection via field ionization, and the quantum systems can be individually addressed as they are separated by centimeter-scale distances [11,16]. In the optical domain, high finesse Fabry–Perot microcavities have been successfully used to realize a strong interaction between the mode of the cavity and cold atoms falling from a magneto-optical trap into a cavity. In this experiment, the presence of atom inside the cavity is detected in real time by high-efficiency measurement via homodyne or heterodyne detection [17]. Generally, single atoms trapped in and coupled to optical resonators hold great promise in applications in quantum networks and quantum communication, as they provide an interface between computation and communication [18–20].

A quantum logic gate is the basic element of a quantum computer. In a quantum network, a set of entangling two-qubit gates with a one-qubit rotation gate is universal for quantum computation [21,22]. For the construction of quantum computation, multiqubit quantum gates play an important role (e.g., they are useful in quantum algorithms and in implementing quantum error correction protocols [23,24]). As the decomposition of multiqubit gates into elementary gates results in a complexity of the N-qubit gates (for instance, in [25] a three-qubit quantum phase gate should be decomposed into five two-qubit quantum phase gates and four one-qubit gates), direct implementation of multiqubit gates is therefore useful to reduce the complexity of the physical realization of practical computation [26]. Several physical systems have been proposed for direct implementations of multiqubit quantum phase gates (see for example [7,11,27–33]).

In this paper, based on cavity QED of free atoms, we theoretically investigate the direct implementation of a three-qubit phase gate in which a four-level atom in a double-V configuration strongly interacts with a high-Q three-mode cavity. The structure of the paper is as follows. In Sect. 2, we give the physical model, use the multiphoton resonance theory for the implementation of a three-qubit quantum phase gate, and then examine the robustness of the scheme to variations in significant parameters of the model. The variation in the gate fidelity due to decoherence processes is presented in Sect. 3, and the possibility to extend the scheme to multiqubit phase gates is discussed. Finally, we conclude the paper in Sect. 4 with a summary.

Fig. 1 The schematic of three-qubit phase gate, where a four-level atom in a double-V type interacts with a three-mode high Q cavity. The cavity can hold three modes of frequencies ω_1, ω_2, and ω_3. The atomic levels are such that $\omega_{e_1g} = \omega_1 + \Delta_1$, $\omega_{e_2g} = \omega_2 + \Delta_2$, and $\omega_{e_3g} = \omega_3 + \Delta_3$
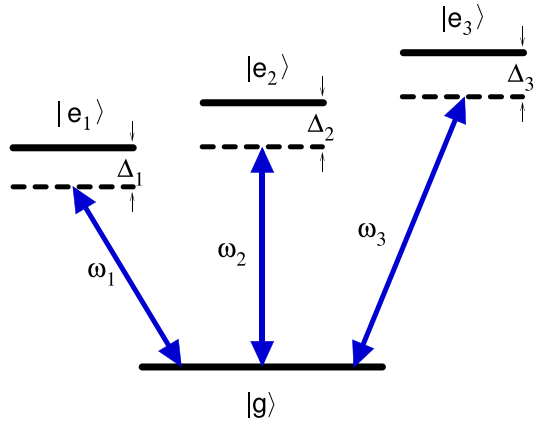
2 Three-qubit quantum phase gate

2.1 Model configuration

A scheme of a three-qubit phase gate is depicted in Fig. 1. This scheme consists of a four-level atom in a double V-configuration of the energy levels (i.e., three excited states $|e_1\rangle$, $|e_2\rangle$, and $|e_3\rangle$ are each coupled to the ground state $|g\rangle$ via a dipole allowed transition but not to each other) inside a three-mode high Q cavity. As shown in Fig. 1, the cavity modes have the resonant frequencies ω_1, ω_2, and ω_3 and the atomic levels are such that $\omega_{e_1g} = \omega_1 + \Delta_1$, $\omega_{e_2g} = \omega_2 + \Delta_2$, and $\omega_{e_3g} = \omega_3 + \Delta_3$.

In the scheme, by choosing photonic qubits to carry quantum information the cavity has three qubits that are encoded in the Fock states $|0\rangle$ and $|1\rangle$. All the possible states in the cavity field therefore are $|0_1, 0_2, 0_3\rangle$, $|1_1, 0_2, 0_3\rangle$, $|0_1, 1_2, 0_3\rangle$, $|0_1, 0_2, 1_3\rangle$, $|1_1, 1_2, 0_3\rangle$, $|1_1, 0_2, 1_3\rangle$, $|0_1, 1_2, 1_3\rangle$, and $|1_1, 1_2, 1_3\rangle$. For a three-qubit phase gate with phase ϕ, we define the operator $\mathscr{T}_\phi$ that describes such a gate via

$$
\begin{aligned}
\mathscr{T}_\phi = &|0_1, 0_2, 0_3\rangle\langle 0_1, 0_2, 0_3| + |1_1, 0_2, 0_3\rangle\langle 1_1, 0_2, 0_3| \\
&+ |0_1, 1_2, 0_3\rangle\langle 0_1, 1_2, 0_3| + |0_1, 0_2, 1_3\rangle\langle 0_1, 0_2, 1_3| \\
&+ |1_1, 1_2, 0_3\rangle\langle 1_1, 1_2, 0_3| + |1_1, 0_2 1_3\rangle\langle 1_1, 0_2 1_3| \\
&+ |0_1, 1_2, 1_3\rangle\langle 0_1, 1_2, 1_3| + \exp(i\phi)|1_1, 1_2, 1_3\rangle\langle 1_1, 1_2, 1_3|,
\end{aligned} \tag{1}
$$

and by setting $\phi = \pi$, a three-qubit quantum phase gate can be realized.

The atom is considered to be in the ground state $|g\rangle$ in and out the cavity. That is, we assume a de-excited atom enters and then leaves the three-qubit cavity in its ground state, such an advantage provides a simple error correction. On exit from the cavity, if the atomic state is not detected to be in the ground state $|g\rangle$ the logic operation must be aborted.

In this paper, we adopt the notation $|a\rangle \otimes |b_1\rangle \otimes |b_2\rangle \otimes |b_3\rangle \equiv |a, b_1, b_2, b_3\rangle$ where, respectively, $|a\rangle (a = g, e_1, e_2, e_3)$ represents atomic state while $|b_i\rangle$ (for $i = 1, 2, 3$) denotes that cavity fields have b photon in mode i with ($b \in 0, 1$). For an atom in

its ground state $|g\rangle$ moving through the cavity, the initial state therefore is $|\psi(0)\rangle = |g, b_1, b_2, b_3\rangle$. It is obvious that the initial state $|g, 0_1, 0_2, 0_3\rangle$ does not evolve with the time. The situation, however, is nontrivial for the initial cavity states other than $|0_1, 0_2, 0_3\rangle$. In the following, we discuss a cavity QED implementation with the case $\phi = \pi$ and all other cavity states are in their initial states.

In the Schrödinger picture and with the dipole and rotating-wave approximations, the Hamiltonian describes the system in Fig. 1 can be written as

$$H = \hbar \sum_{i=g,e_1,e_2,e_3} \omega_i \hat{\sigma}_{ii} + \hbar \sum_{j=1}^{3} \omega_j \hat{a}_j^\dagger \hat{a}_j$$
$$+ \hbar[g_1 \hat{a}_1 \hat{\sigma}_{e_1 g} + g_2 \hat{\sigma}_{ge_2} \hat{a}_2^\dagger + g_3 \hat{a}_3 \hat{\sigma}_{e_3 g} + \text{H.c.}], \qquad (2)$$

where the coupling strengths are $g_j (j = 1, 2, 3)$, the atomic operators $\hat{\sigma}_{e_1 g} \equiv |e_1\rangle\langle g|$, $\hat{\sigma}_{ge_2} \equiv |g\rangle\langle e_2|$, and $\hat{\sigma}_{e_3 g} \equiv |e_3\rangle\langle g|$, and $\hat{a}_j$ is the photon annihilation operator for the cavity mode.

2.2 Effective Hamiltonian

We now apply the theory of multiphoton resonance developed by Shore in [34] so that the three-qubit phase gate in Eq. (1) is implemented. This theory, in general, has been used in earlier works [35,36] for the implementation of a set of universal gates. For a detailed study of the multiphoton process in cavity QED see [37]. In this paper, we actually improve and extend the method to the implementation of a three-qubit and more generally a multiqubit quantum phase gate. Following Shore's theory, we first introduce two orthogonal projection operators P and Q where $P + Q = 1$, $PP = P$, $QQ = Q$, and $PQ = QP = 0$. Throughout this work, we assume the states of interest to correspond the subsystem spanned by P, leaving the remaining states in the Q subsystem. The cavity field frequencies ω_1 and ω_2 (see Fig. 1) are assumed to be far detuned from the energy differences of the ground state $|g\rangle$ and then the states $|e_1\rangle$ and $|e_2\rangle$ are spanned by Q, but the cavity field frequency ω_3 is appropriately detuned from the energy difference of $|g\rangle$ and therefore a two-level behavior occurs between levels $|g\rangle$ and $|e_3\rangle$. The two-level effective Hamiltonian describing the subsystem $|\psi\rangle_P$ can be defined as $H_{\text{eff}} = H_0 - BA^{-1}B^\dagger$ where $H_0 = PH_I P$, $A = QH_I Q$, $B = PH_I Q$, and H_I is the Hamiltonian describing a system in an interaction picture. In the following, we will find that the logical states $|1_1, 0_2, 0_3\rangle$, $|0_1, 1_2, 0_3\rangle$, $|0_1, 0_2, 1_3\rangle$, $|1_1, 1_2, 0_3\rangle$ remain in their initial states as a result of choosing appropriate values for detunings, the global phases, and the gate operation time. The interesting situations are, however, when the initial states are $|g, 1_1, 1_2, 1_3\rangle$, $|g, 1_1, 0_2, 1_3\rangle$, and $|g, 0_1, 1_2, 1_3\rangle$. For such initial states, we apply Shore's method [34] to determine the proper values for the resonance conditions so that the condition for $\mathcal{T}_\phi$ is realized.

2.2.1 Input state: $|g, 1_1, 1_2, 1_3\rangle$

For an atom with such a configuration (see Fig. 1) in its ground state $|g\rangle$ moving through the cavity with three photons in its modes, the initial state then is $|\psi(0)\rangle = |g, 1_1, 1_2, 1_3\rangle$ and after interaction time t, the state of the system is given by

$$|\psi(t)\rangle = \beta_1(t)|g, 1_1, 1_2, 1_3\rangle + \beta_2(t)|e_1, 0_1, 1_2, 1_3\rangle$$
$$+ \beta_3(t)|e_2, 1_1, 0_2, 1_3\rangle + \beta_4(t)|e_3, 1_1, 1_2, 0_3\rangle, \tag{3}$$

and therefore the Hamiltonian describing this system in an interaction picture can take the form ($\hbar = 1$)

$$
\begin{aligned}
H_I = {} & \Delta_1 |e_1, 0_1, 1_2, 1_3\rangle\langle e_1, 0_1, 1_2, 1_3| \\
& + \Delta_2 |e_2, 1_1, 0_2, 1_3\rangle\langle e_2, 1_1, 0_2, 1_3| \\
& + \Delta_3 |e_3, 1_1, 1_2, 0_3\rangle\langle e_3, 1_1, 1_2, 0_3| \\
& + [g_1 |e_1, 0_1, 1_2, 1_3\rangle\langle g, 1_1, 1_2, 1_3| \\
& + g_2 |g, 1_1, 1_2, 1_3\rangle\langle e_2, 1_1, 0_2, 1_3| \\
& + g_3 |e_3, 1_1, 1_2, 0_3\rangle\langle g, 1_1, 1_2, 1_3| + \text{H.c.}],
\end{aligned}
\tag{4}
$$

with $\Delta_1 = [(\omega_{e_1} - \omega_g) - \omega_1]$, $\Delta_2 = [(\omega_{e_2} - \omega_g) - \omega_2]$, and $\Delta_3 = [(\omega_{e_3} - \omega_g) - \omega_3]$.

We consider the case in which $|e_1\rangle$ and $|e_2\rangle$ are always set to be far from resonance and the states of interest correspond to the subsystem $|\psi\rangle_P$ spanned by P, $|\psi\rangle_P = \beta_1(t)|g, 1_1, 1_2, 1_3\rangle + \beta_4(t)|e_3, 1_1, 1_2, 0_3\rangle$. In this case, Δ_1 and $\Delta_2 \gg g_j$ with $g_j (j = 1, 2, 3)$ are all of the coupling constants, whereas Δ_3 to be small and its proper value will be determined later to ensure resonance. We use the two-level effective Hamiltonian defined by $H_{\text{eff}} = H_0 - BA^{-1}B^\dagger$ where $H_0 = PH_IP$, $A = QH_IQ$, $B = PH_IQ$, and H_I is given by Eq. (4). For reasons of convenience, the Hamiltonian in Eq. (4) is rewritten in the matrix framework. That is, in the basis $\{|g, 1_1, 1_2, 1_3\rangle, |e_1, 0_1, 1_2, 1_3\rangle, |e_2, 1_1, 0_2, 1_3\rangle, |e_3, 1_1, 1_2, 0_3\rangle\}$ one can represent H_I as

$$
H_I = \begin{bmatrix}
0 & g_1 & g_2 & g_3 \\
g_1 & \Delta_1 & 0 & 0 \\
g_2 & 0 & \Delta_2 & 0 \\
g_3 & 0 & 0 & \Delta_3
\end{bmatrix}.
\tag{5}
$$

Selecting states $|g, 1_1, 1_2, 1_3\rangle$ and $|e_3, 1_1, 1_2, 0_3\rangle$ as our P space, one can then partition H_I into the matrices:

$$
B = \begin{bmatrix} g_1 & g_2 \\ 0 & 0 \end{bmatrix}, \; H_0 = \begin{bmatrix} 0 & g_3 \\ g_3 & \Delta_3 \end{bmatrix}, \; A = \begin{bmatrix} \Delta_1 & 0 \\ 0 & \Delta_2 \end{bmatrix}.
\tag{6}
$$

Using these parts and after a trivial energy shift, the effective two-level Hamiltonian is
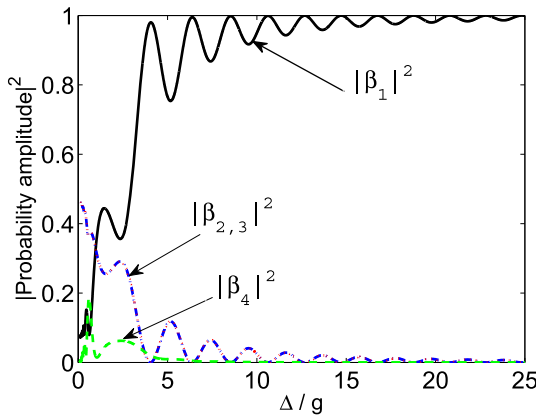
Fig. 2 Populations for the four-state system (3) as a function of normalized detuning Δ/g, where the two-level behavior of Eqs. (8) and (9) are used for parameters in the Hamiltonian (4). Parameters: the coupling strengths g_i ($i = 1, 2, 3$) are all set to g, the detunings Δ_1 and Δ_2 are set to Δ, and the value of Δ_3 is determined by the resonance condition in Eq. (9). In this plot, solid line is $|\beta_1|^2$, $|\beta_2|^2$ and $|\beta_3|^2$ are represented by dotted and dash-dot lines, and $|\beta_4|^2$ is the dashed line

$$H_{\text{eff}} = g_{\text{eff}} \, (\hat{\sigma}^- + \hat{\sigma}^+) + \Delta_{\text{eff}} \, \hat{\sigma}^+ \hat{\sigma}^-, \tag{7}$$

where the operators $\hat{\sigma}^- \equiv |g, 1_1, 1_2, 1_3\rangle\langle e_3, 1_1, 1_2, 0_3|$ and $\hat{\sigma}^+ \equiv |e_3, 1_1, 1_2, 0_3\rangle$ $\langle g, 1_1, 1_2, 1_3|$. The effective coupling g_{eff} and the resonance condition Δ_3 (by setting $\Delta_{\text{eff}} = 0$) are determined by

$$g_{\text{eff}} = g_3, \tag{8}$$

$$\Delta_{\text{eff}} = \Delta_3 + g_1^2/\Delta_1 + g_2^2/\Delta_2. \tag{9}$$

The time evolution of the system for the states of interest is thus given by

$$|g, 1_1, 1_2, 1_3\rangle \mapsto \cos(g_{\text{eff}}t) \, |g, 1_1, 1_2, 1_3\rangle$$
$$- i \sin(g_{\text{eff}}t) \, |e_3, 1_1, 1_2, 0_3\rangle. \tag{10}$$

By setting the time evolution to ($|g_{\text{eff}}t| = \pi$) a π shift for the state $|1_1, 1_2, 1_3\rangle$ is introduced. In Fig. 2 and by numerically integrating the full Hamiltonian (4), we plot the populations for the four-state system in Eq. (3) as a function in Δ/g with the use of the parameters in Eqs. (8) and (9) at $|g_{\text{eff}}t| = \pi$. This plot shows the exact numerical dynamics to the analytical behavior in Eq. (10).

2.2.2 Input states: $|g, 1_1, 0_2, 1_3\rangle$ and $|g, 0_1, 1_2, 1_3\rangle$

We now consider the situation in which the input states are $|g, 1_1, 0_2, 1_3\rangle$ and $|g, 0_1, 1_2, 1_3\rangle$. For the system initially in the state $|g, 1_1, 0_2, 1_3\rangle$, the state of the system at any time t is given by

$$|\psi(t)\rangle = \xi_1(t)|g, 1_1, 0_2, 1_3\rangle + \xi_2(t)|e_1, 0_1, 0_2, 1_3\rangle$$
$$+ \xi_3(t)|e_3, 1_1, 0_2, 0_3\rangle. \tag{11}$$

The Hamiltonian that describes the system in Eq. (11) in an interaction picture can be then given by

$$
\begin{aligned}
H_I = {}& \Delta_1|e_1, 0_1, 0_2, 1_3\rangle\langle e_1, 0_1, 0_2, 1_3| \\
& + \Delta_3|e_3, 1_1, 0_2, 0_3\rangle\langle e_3, 1_1, 0_2, 0_3| \\
& + [g_1|e_1, 0_1, 0_2, 1_3\rangle\langle g, 1_1, 0_2, 1_3| \\
& + g_3|g, 1_1, 0_2, 1_3\rangle\langle e_3, 1_1, 0_2, 0_3| + \text{H.c.}],
\end{aligned}
\tag{12}
$$

with $\Delta_1 = [(\omega_{e_1} - \omega_g) - \omega_1]$ and $\Delta_3 = [(\omega_{e_3} - \omega_g) - \omega_3]$.

Following the same procedure outlined in the previous section, the operator P projects onto the states we select to be populated: $|g, 1_1, 0_2, 1_3\rangle$ and $|e_3, 1_1, 0_2, 0_3\rangle$. The operator Q therefore projects onto the state $|e_1, 0_1, 0_2, 1_3\rangle$. The Hamiltonian (12) can be displayed as the matrix

$$
H_I = \begin{bmatrix} 0 & g_1 & g_3 \\ g_1 & \Delta_1 & 0 \\ g_3 & 0 & \Delta_3 \end{bmatrix},
\tag{13}
$$

and then one can partition H_I into the following operators:

$$
B = \begin{bmatrix} g_1 \\ 0 \end{bmatrix}, \; H_0 = \begin{bmatrix} 0 & g_3 \\ g_3 & \Delta_3 \end{bmatrix}, \; A = \Delta_1.
\tag{14}
$$

Using these parts and according to the definition of the two-state effective Hamiltonian, i.e., $H_{\text{eff}} = H_0 - BA^{-1}B^\dagger$, the effective coupling constant and the resonance condition can be then determined by

$$g_{\text{eff}} = g_3, \tag{15}$$
$$\Delta_{\text{eff}} = \Delta_3 + g_1^2/\Delta_1. \tag{16}$$

Therefore, the two-level system $|\psi(t)\rangle_P = \xi_1(t)|g, 1_1, 0_2, 1_3\rangle + \xi_3(t)|e_3, 1_1, 0_2, 0_3\rangle$ evolves in time as

$$|g, 1_1, 0_2, 1_3\rangle \mapsto \cos(g_{\text{eff}}t) \, |g, 1_1, 0_2, 1_3\rangle$$
$$- i \sin(g_{\text{eff}}t) \, |e_3, 1_1, 0_2, 0_3\rangle. \tag{17}$$

Similarly, for the input state $|g, 0_1, 1_2, 1_3\rangle$ and after interaction time t, one finds that this state evolves as

$$|\psi(t)\rangle = \lambda_1(t)|g, 0_1, 1_2, 1_3\rangle + \lambda_2(t)|e_2, 0_1, 0_2, 1_3\rangle$$
$$+ \lambda_3(t)|e_3, 0_1, 1_2, 0_3\rangle, \tag{18}$$

and the Hamiltonian describing this system in an interaction picture can be represented as

$$
\begin{aligned}
H_I = {} & \Delta_2 |e_2, 0_1, 0_2, 1_3\rangle\langle e_2, 0_1, 0_2, 1_3| \\
& + \Delta_3 |e_3, 0_1, 1_2, 0_3\rangle\langle e_3, 0_1, 1_2, 0_3| \\
& + [g_2 |e_2, 0_1, 0_2, 1_3\rangle\langle g, 0_1, 1_2, 1_3| \\
& + g_3 |g, 0_1, 1_2, 1_3\rangle\langle e_3, 0_1, 1_2, 0_3| + \text{H.c.}],
\end{aligned}
\tag{19}
$$

with $\Delta_2 = [(\omega_{e_2} - \omega_g) - \omega_2]$ and $\Delta_3 = [(\omega_{e_3} - \omega_g) - \omega_3]$.

Selecting out the states $|g, 0_1, 1_2, 1_3\rangle$ and $|e_3, 0_1, 1_2, 0_3\rangle$ to be close to resonance and then to be spanned by P, the resultant operators B, H_0, and A which are required for constructing the effective Hamiltonian $H_{\text{eff}} = H_0 - BA^{-1}B^\dagger$ are

$$
B = \begin{bmatrix} g_2 \\ 0 \end{bmatrix}, \ H_0 = \begin{bmatrix} 0 & g_3 \\ g_3 & \Delta_3 \end{bmatrix}, \ A = \Delta_2.
\tag{20}
$$

The parameters of the effective coupling constant g_{eff} and the effective detuning Δ_{eff} for the resultant two-level behavior are

$$
g_{\text{eff}} = g_3,
\tag{21}
$$

$$
\Delta_{\text{eff}} = \Delta_3 + g_2^2/\Delta_2.
\tag{22}
$$

The dynamical evolution of the state $|\psi(t)\rangle_P = \lambda_1(t)|g, 0_1, 1_2, 1_3\rangle + \lambda_3(t)|e_3, 0_1, 1_2, 0_3\rangle$ can be given then as

$$
\begin{aligned}
|g, 0_1, 1_2, 1_3\rangle \mapsto {} & \cos(g_{\text{eff}}t) \, |g, 0_1, 1_2, 1_3\rangle \\
& - i \sin(g_{\text{eff}}t) \, |e_3, 0_1, 1_2, 0_3\rangle.
\end{aligned}
\tag{23}
$$

Choosing an interaction time ($|g_{\text{eff}}t| = \pi$) for both the state $|g, 1_1, 0_2, 1_3\rangle$ in Eq. (17) and the state $|g, 0_1, 1_2, 1_3\rangle$ in Eq. (23), the logical states $|1_1, 0_2, 1_3\rangle$ and $|0_1, 1_2, 1_3\rangle$ remain unaffected (note that we can, in principle, consider a global phase such that undesired phase factor is removed [38]). This completes the description of the three-qubit phase gate $\mathscr{T}_\phi$.

To check the validity of our proposal, we numerically integrate the full Hamiltonians in Eqs. (4), (12), and (19) and measure the variation of the fidelity of the gate $\mathscr{T}_\phi$. For different values of a detuning $\Delta = \Delta_i$ (with $i = 1, 2$), Fig. 3 shows the variation of the fidelity for the systems (3), (11), and (18) for being in the qubit states $|g, 1_1, 1_2, 1_3\rangle$, $|g, 1_1, 0_2, 1_3\rangle$, and $|g, 0_1, 1_2, 1_3\rangle$, respectively. It is clear that fidelities oscillate with peak values close to $F = 1$ for the value of a detuning $\Delta \geqslant 4g$. Moreover, in Fig. 4 and for the same systems, we allow the values of Δ_3 to vary slightly around the resonance conditions in Eqs. (9), (16), and (22) and measure the variation in fidelity. The inset in this figure shows the effect of the variation of the atom-field strength in order of 2%. It is apparent that these systems are reasonably insensitive to variations in such parameters. Under the conditions $\Delta_{1,2} \gg \Delta_3, g_i$ (for $i = 1, 2, 3$) and the interaction
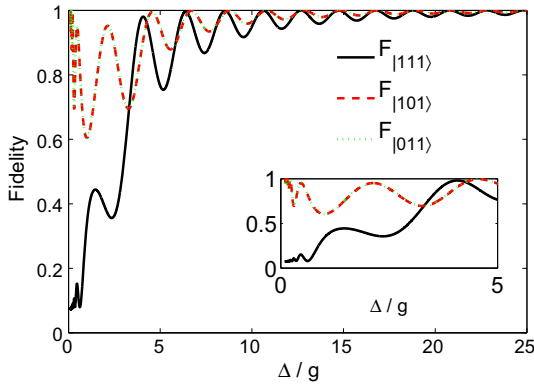
Fig. 3 Variation of the fidelity F versus normalized Δ/g. The procedure of the effective two-level Hamiltonian is utilized to measure the fidelity for the systems (3), (11), and (18). Parameters: all coupling constants g_i (for $i = 1, 2, 3$) are set to g, the detunings Δ_1 and Δ_2 are set to Δ. The values for Δ_3 are determined by the resonance conditions in Eqs. (9), (16), and (22) for the systems (3), (11), and (18), respectively. Zoom shows the fidelity F in the region $0 < \Delta/g \leq 5$ for the same parameters
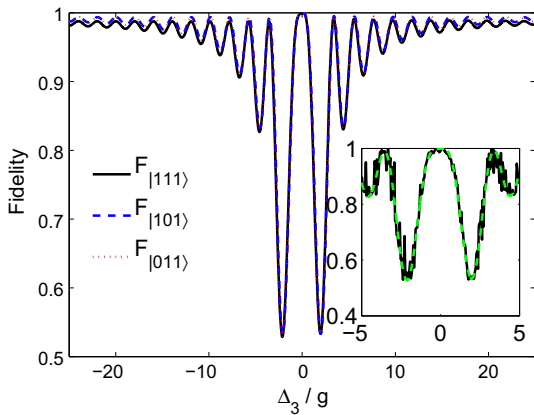
Fig. 4 Variation of the fidelity F for the systems (3), (11), and (18) as function of Δ_3/g. Parameters: the coupling strengths g_i for ($i = 1, 2, 3$) are all set to g, the values of Δ_1 and Δ_2 are set to Δ with $\Delta = 25g$, and the value of Δ_3 is determined by the resonance conditions (9), (16), and (22). The inset measures the variation of F for the system (3) for the same parameters, when slightly deviation in the coupling constants g is considered

time between the field and the atom ($|g_{\text{eff}}t| = \pi$), the other logical qubits $|1_1, 0_2, 0_3\rangle$, $|0_1, 1_2, 0_3\rangle$, $|0_1, 0_2, 1_3\rangle$, $|1_1, 1_2, 0_3\rangle$ remain unaltered.

3 Effects of decoherence

Since decoherence is a strong limiting factor in the implementation of any quantum gate operation, it is necessary to measure the robustness of the three-qubit gate $\mathscr{T}_\phi$ with a consideration of such a factor. In what follows, we measure the variation in the

gate fidelity when the dissipative processes, namely via photonic and atomic decays, need to be considered. We only give the detail analysis of the influence of decoherence processes when the initial state is $|g, 1_1, 1_2, 1_3\rangle$.

For this purpose, we use two different treatments: the density matrix approach as a numerical method and the wave function approach as an analytical method. Beginning with the numerical treatment, we recall Liouville's equation (or general master equation) that can be written, in the density matrix framework, as

$$\frac{\partial}{\partial t}\rho = -i[H_I, \rho] + \mathscr{L}\rho. \tag{24}$$

The first term in Eq. (24) describes the atom-field coupling for the system H_I in Eq. (4) and the second term $\mathscr{L}\rho$ is known as Liouville's operator and contains the effects of dissipations. At zero temperature, the Liouvillian $\mathscr{L}\rho$ has the so-called Lindblad form [39]

$$\mathscr{L}\rho = \sum_i \eta_i \, \mathcal{D}_i \rho \mathcal{D}_i^\dagger - \frac{1}{2}\sum_i \eta_i (\mathcal{D}_i^\dagger \mathcal{D}_i \rho + \rho \mathcal{D}_i^\dagger \mathcal{D}_i), \tag{25}$$

where η represents the loss of population. In our case, we consider two dominant channels for decoherence mechanisms, namely the spontaneous emission γ and the cavity field rate κ. The operators $\mathcal{D}$ and $\mathcal{D}^\dagger$ are the corresponding system operators. In Fig. 5, we use Liouville's equation, and under the existence of atomic and photonic decays, we numerically integrate the full Hamiltonian (4) to measure the impact of dissipative processes on the gate fidelity. This figure shows that the gate fidelity remains above 0.90 for the parameters $\kappa = 0.003g$ and $\gamma = 0.005g$. In the view of recent cavity QED experiments, the gate fidelity becomes $F \sim 1$. For example, in the experiment
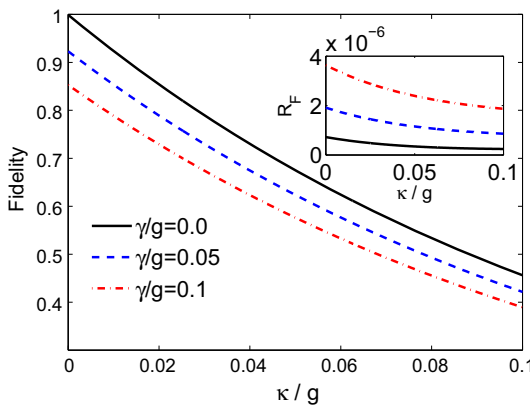
Fig. 5 Variation of the fidelity F for the system (3) in the presence of atomic and photonic decays. Parameters: the coupling strengths g_i for ($i = 1, 2, 3$) are all set to g, the values of Δ_1 and Δ_2 are set to Δ with $\Delta = 25g$, and the value of Δ_3 is determined by the resonance condition (9). The inset measures the deviations between theoretical and numerical results by calculating the relative fidelity R_F as a function of the fraction κ/g

[40], where $\gamma/g = 0.0001$ and $\gamma = 4\kappa$, the gate fidelity is $F > 0.999$. The system, therefore, is substantially insensitive to variations in such parameters.

We now seek to deeply understand the numerical results provided by the density matrix approach in Eq. (24) by deriving analytical solutions. To this end, we use the wave function method in [41]. Applying the Lindblad Form in Eq. (25) on the system (3) shows that this system is not closed and decay channels result in the irreversible loss of population. The system for the states of interest $|\psi(t)\rangle_P = c_g|g, 1_1, 1_2, 1_3\rangle + c_{e_3}|e_3, 1_1, 1_2, 0_3\rangle$, therefore, can be described by the non-Hermitian Hamiltonian

$$H'_{\text{eff}} = -\frac{i}{2}(\kappa_1 + \kappa_2 + \kappa_3))\,\hat{\sigma}^-\hat{\sigma}^+ + g_{\text{eff}}\,(\hat{\sigma}^- + \hat{\sigma}^+)$$
$$+ (\Delta_{\text{eff}} - \frac{i}{2}(\gamma_{e_3g} + \kappa_1 + \kappa_2))\,\hat{\sigma}^+\hat{\sigma}^-, \tag{26}$$

where κ_i with $(i = 1, 2, 3)$ and γ_{e_3g} denote the cavity field and the atomic relaxations, respectively, and the definitions of the operators σ^- and σ^+ can be found in Eq. (7). One, thus, can propagate the state vector $|\psi(t)\rangle_P$ with the Schrödinger equation using H'_{eff}, which yields the following differential equations (with $g_{\text{eff}} = g_3$ and assuming exact resonance, $\Delta_{\text{eff}} = 0$)

$$\frac{\partial}{\partial t}c_g = -\frac{1}{2}(\kappa_1 + \kappa_2 + \kappa_3)\,c_g - i\,g_3\,c_{e_3},$$
$$\frac{\partial}{\partial t}c_{e_3} = -i\,g_3\,c_g - \frac{1}{2}(\gamma_{e_3g} + \kappa_1 + \kappa_2)\,c_{e_3}. \tag{27}$$

With initial conditions ($c_g(t = 0) = 1$ and $c_{e_3}(t = 0) = 0$) and in the strong coupling regime $g_3 > \kappa, \gamma$ (note that $\kappa_i = \kappa$ (for $i = 1, 2, 3$) and $\gamma_{e_3g} = \gamma$), the solutions for ($c_g(t)$ and $c_{e_3}(t)$) can be then given as

$$|\psi(t)\rangle_P = \left\{ \left[\cos(g_3 t) + \frac{(\gamma - \kappa)}{4g_3}\,\sin(g_3 t)\right]|g, 1_1, 1_2, 1_3\rangle \right.$$
$$\left. - i\,\sin(g_3 t)|e_3, 1_1, 1_2, 0_3\rangle \right\}\exp-\left(\frac{(\gamma + 5\kappa)}{4}t\right). \tag{28}$$

The fidelity of the system $|\psi(t = \pi/g_3)\rangle_P$, therefore, decreases according to $F \sim e^{-\frac{\pi}{2}(\frac{\gamma + 5\kappa}{g_3})}$. In the presence of dissipation processes, the deviation between analytical and numerical calculations is depicted in the inset in Fig. 5 and measured by the quantity of relative fidelity R_F, such a quantity can be defined as $R_F = |F_{\text{th}} - F_{\text{num}}|/F_{\text{num}}$ where F_{th} is the fidelity calculated by Eq. (28) and F_{num} is the system fidelity given by the numerical integration of the full Hamiltonian (4). This plot clearly indicates the agreement between the results provided by the use of the density operator method and the wave function approach.

For the input states $|g, 1_1, 0_2, 0_3\rangle$, $|g, 0_1, 1_2, 0_3\rangle$, $|g, 0_1, 0_2, 1_3\rangle$, $|g, 1_1, 1_2, 0_3\rangle$, $|g, 1_1, 0_2, 1_3\rangle$, and $|g, 0_1, 1_2, 1_3\rangle$ either density matrix treatment, wave function

method or both can be used to study the effects of atomic and cavity decays on the populations of these initial states. It is also observed that the system in each input state is not closed and it decays via the atomic spontaneous emission with the rate γ and via the cavity field relaxation with the rate κ. Moreover, we find that decay channels in all these systems result in an irreversible loss of population. In what follows, we measure, if necessary, the impact of the decoherence processes for these input states by integrating Eq. (24).

We now discuss the feasibility of implementing the proposed scheme within recent cavity QED techniques. Our scheme explicitly requires the cavity modes ω_1 and ω_2 to be far detuned from the atomic transition frequencies $\omega_{e_1 g}$ and $\omega_{e_2 g}$, respectively, and the cavity mode ω_3 to be nearly resonant with $\omega_{e_3 g}$. The sharp value of Δ_3 is determined by the resonance conditions. These requirements demand high control of the values of significant parameters such as couplings and detunings. Recently, this kind of control has been demonstrated by numerous cavity QED experiments. For example, it is illustrated in [40] that for Rb^{85} atoms passing through a microwave cavity and by using pulsed velocity-selected samples, the atomic position is known at any time and the atoms are set in resonance during a short time window at a well defined position in the cavity. For the case where a multilevel atom interacting with a multimode cavity, it is reported in [42] that cold atoms such as Rb^{87} were positioned at the cavity center within $4 \, \mu m$.

The scheme proposed here also requires the atom–cavity interaction to be in a strong coupling regime. The strong coupling realization has been achieved by various cavity QED techniques. For instance, in an experiment performed by [40] circular Rydberg atoms with radiative lifetimes of the order of $T_{at} = 30$ ms enter a microwave cavity with ultrahigh Q factor approaching 4.2×10^{10} and with a damping time $T_c = 130$ ms at 51 GHz, where the coupling constant for the atom–cavity interaction system is $g/2\pi = 47$ kHz. This experiment certainly works in the strong coupling regime (i.e., $g > \gamma, \kappa$). Considering such an experiment and as we have previously found for the three-qubit quantum phase gate discussed here that the interaction time required to realize the gate is $gT_{int} = \pi$, the three relevant times are $(T_{int}, T_{at}, T_c) \sim (0.01, 30, 130)$ ms. It is, therefore, apparent that the relaxation times T_{at} and T_c are much longer than the atom–cavity interaction time of the present scheme (slow decoherence and fast gate operation), and therefore, all requirements for implementing the scheme are satisfied.

It is worth noting that we can easily extend our scheme to realize multiqubit quantum phase gates. The theory of multiphoton resonance can generally be used to isolate two-level behavior from the general N-level rotating-wave approximation Schrödinger equation. By adding more transitions to the three-qubit phase gate configuration (see Fig. 1) and by the use of multiphoton resonance theory, one can therefore actually construct the two-level behavior between the initial state $|g, 1_1, 1_2, \ldots, 1_{N-1}, 1_N\rangle$ and the last state of a sequence $|e_N, 1_1, 1_2, \ldots, 1_{N-1}, 0_N\rangle$. Building the effective two-level Hamiltonians, we can then precisely determine the proper values for the resonance conditions, the effective couplings, and the interaction time in which the phase shift is induced on the initial state, and therefore, the gate operation can be formed. Additionally, impacts of decoherence in the implementation of the resultant multiqubit gate can be addressed by the use of both the density matrix approach and wave function method, by following the same procedure described in Sec. 3.

4 Conclusion

In summary, we have presented a scheme for realizing a three-qubit quantum phase gate in which a four-level double V-type atom strongly interacts with a high-Q three-mode cavity. The technique of adiabatic elimination from atomic physics is utilized to define the effective two-level Hamiltonians and then to locate the resonances. Some practical considerations such as the effects of deviation in detunings Δ_i (for $i = 1, 2, 3$) and coupling constants g and the influence of the presence of decoherence processes have all been addressed, showing that the proposed scheme is highly insensitive to such variations. We also find that the scheme can be easily extended for direct implementation of multiqubit quantum phase gate.

In the scheme, we consider an interaction between a multilevel atom and a multimode field simultaneously inside a high-Q cavity in the strong coupling regime. Recently, there has been considerable interest in constructing experiments where a strong coupling between a multilevel atom and a multimode cavity is realizable. This kind of interaction is experimentally achievable with the current development in the resonator systems (see for example [42,43]).

The scheme proposed here has the following important features: (i) In the scheme the three qubits are encoded on three modes inside a cavity (each qubit is therefore treated equally), making the scheme favored for the realization of typical quantum algorithms; (ii) the scheme is reasonably insensitive to decoherence processes and the variations in important parameters such as detunings and couplings, meaning that the scheme has reached a practical compromise on sensitivity and gate speed; (iii) as the atom is proposed to be always in the ground state in and out the cavity, this feature forms a simple error correction; (iv) it is possible to theoretically analyze decoherence effects on the system, which provides further details for the population decays from the excited states and the quantum jump events in the system; and (v) the scheme is easily extendable to multiqubit phase gates. In general, the present scheme has a high feasibility with recent or near-future experimental technology, enabling numerous applications in the area of quantum information processing.

References

1. Ladd, T.D., Jelezko, F., Laflamme, R., Nakamura, Y., Monroe, C., O'Brien, J.L.: Quantum computers. Nature **464**, 45–53 (2010)
2. Browne, D., Bose, S., Mintert, F., Kim, M.S.: From quantum optics to quantum technologies. Prog. Quantum Electron. **54**, 2–18 (2017)
3. Shor, P.W.: Polynomial-time algorithms for prime factorization and discrete logarithms on a quantum computer. SIAM J. Comput. **26**(5), 1484–1509 (1997)
4. Grover, L.K.: Quantum mechanics helps in searching for a needle in a haystack. Phys. Rev. Lett. **79**(2), 325–328 (1997)
5. Long, G.L.: Grover algorithm with zero theoretical failure rate. Phys. Rev. A **64**(2), 022307 (2001)
6. Kempe, J., Bacon, D., DiVincenzo, D.P., Whaley, K.: Encoded university from a single physical interaction. Quantum Inf. Comput. **1**(4), 33–55 (2001)

7. Cirac, J.I., Zoller, P.: Quantum computations with cold trapped ions. Phys. Rev. Lett. **74**(20), 4091–4094 (1995)

8. Jonathan, A.J., Michele, M., Rasmus, H.H.: Implementation of a quantum search algorithm on a quantum computer. Nature **393**, 344–346 (1998)

9. Kok, P., Munro, W.J., Nemoto, K., Ralph, T.C., Dowling, J.P., Milburn, G.J.: Linear optical quantum computing with photonic qubits. Rev. Mod. Phys. **79**(1), 135–174 (2007)

10. Hanson, R., Awschalom, D.D.: Coherent manipulation of single spins in semiconductors. Nature **453**, 1043–1049 (2008)

11. Raimond, J.M., Brune, M., Haroche, S.: Manipulating quantum entanglement with atoms and photons in a cavity. Rev. Mod. Phys. **73**(3), 565–582 (2001)

12. Buluta, I., Ashhab, S., Nori, F.: Natural and artificial atoms for quantum computation. Rep. Prog. Phys. **74**(10), 104401 (2011)

13. You, J.Q., Nori, F.: Atomic physics and quantum optics using superconducting circuits. Nature **474**(7353), 589–597 (2011)

14. Mabuchi, H., Doherty, A.C.: Cavity quantum electrodynamics: coherence in context. Science **298**(5597), 1372–1377 (2002)

15. van Enk, S.J., Kimble, H.J., Mabuchi, H.: Quantum information processing in cavity-QED. Quantum Inf. Process. **3**(1–5), 75–90 (2004)

16. Walther, H., Varcoe, B.T.H., Englert, B.G., Becker, T.: Cavity quantum electrodynamics. Rep. Prog. Phys. **69**(5), 1325 (2006)

17. Miller, R., Northup, T.E., Birnbaum, K.M., Boca, A., Boozer, A.D., Kimble, H.J.: Trapped atoms in cavity QED: coupling quantized light and matter. J. Phys. B At. Mol. Opt. Phys. **38**(9), S551 (2005)

18. Reiserer, A., Rempe, G.: Cavity-based quantum networks with single atoms and optical photons. Rev. Mod. Phys. **87**(4), 1379–1418 (2015)

19. Hacker, B., Welte, S., Rempe, G., Ritter, S.: A photon–photon quantum gate based on a single atom in an optical resonator. Nature **536**, 193–196 (2016)

20. O'Brien, J.L., Furusawa, A., Vŭcković,: Photonic quantum technologies. Nat. Photon. **3**, 687–695 (2009)

21. Barenco, A., Bennett, C.H., Cleve, R., DiVincenzo, D.P., Margolus, N., fiShor, P., Sleator, T., Smolin, J.A., Weinfurter, H.: Elementary gates for quantum computation. Phys. Rev. A **52**(5), 3457–3467 (1995)

22. Liu, Y., Long, G.L., Sun, Y.: Analytic one-bit and CNOT gate constractions of general n-qubit controlled gates. Int. J. Quantum Inf. **6**(3), 447–462 (2008)

23. Zubairy, M.S., Matsko, A.B., Scully, M.O.: Resonant enhancement of high-order optical nonlinearities based on atomic coherence. Phys. Rev. A **65**, 043804 (2002)

24. Chiaverini, J., Leibfried, D., Schaetz, T., Barrett, M.D., Blakestad, R.B., Britton, J., Itano, W.M., Jost, J.D., Knill, E., Langer, C., Ozeri, R., Wineland, D.J.: Realization of quantum error correction. Nature **432**, 602–605 (2004)

25. Chang, J.T., Zubairy, M.S.: Three-qubit phase gate based on cavity quantum electrodynamics. Phys. Rev. A **77**(1), 012329 (2008)

26. Vedral, V., Barenco, A., Ekert, A.: Quantum networks for elementary arithmetic operations. Phys. Rev. A **54**(1), 147 (1996)

27. Zhang, J., Liu, W., Deng, Z., Lu, Z., Long, G.L.: Modularization of a multi-qubit controlled phase gate and its nuclear magnetic resonance implementation. J. Opt. B Quantum Semiclass. Opt. **7**(1), 22 (2004)

28. Zou, X., Li, K., Guo, G.: Linear optical scheme for direct implementation of a nondestructive N-qubit controlled phase gate. Phys. Rev. A **74**, 044305 (2006)

29. Wang, X., Sørensen, A., Mølmer, K.: Multibit gates for quantum computing. Phys. Rev. Lett. **86**(17), 3907–3910 (2001)

30. Yang, C.-P., Zheng, S.-B., Nori, F.: Multiqubit tunable phase gate of one qubit simultaneously controlling *n* qubits in a cavity. Phys. Rev. A **82**(6), 062326 (2010)

31. Yang, C.-P., Liu, Y.-X., Nori, F.: Phase gate of one qubit simultaneously controlling *n* qubits in a cavity. Phys. Rev. A **81**(6), 062323 (2010)

32. Ye, B., Zheng, Z.-F., Yang, C.-P.: Multiplex-controlled phase gate with qubits distributed in a multi-cavity system. Phys. Rev. A **97**(6), 062336 (2018)

33. Fan, Y.-J., Zheng, Z.-F., Zhang, Y., Lu, D.-M., Yang, C.-P.: One-step implementation of a multi-target-qubit controlled phase gate with cat-state qubits in circuit QED. Front. Phys. **14**(2), 21602 (2019)

34. Shore, B.W.: Two-level behavior of coherent excitation of multilevel systems. Phys. Rev. A **24**(3), 1413–1418 (1981)
35. Everitt, M.S., Garraway, B.M.: Multiphoton resonances for all-optical quantum logic with multiple cavities. Phys. Rev. A **90**(1), 012335 (2014)
36. Alqahtani, M.M.: Quantum phase gate based on multiphoton process in multimode cavity QED. Quantum Inf. Process. 17(9). https://doi.org/10.1007/s11128-018-1979-6
37. Liu, Y.-X., You, J.Q., Wei, L.F., Sun, C.P., Nori, F.: Optical selection rules and phase-dependent adiabatic state control in a superconducting quantum circuit. Phys. Rev. Lett. **95**(8), 087001 (2005)
38. Nielsen, M.A., Chuang, I.L.: Quantum Computation and Quantum Information. Cambridge University Press, Cambridge (2000)
39. Lindblad, G.: On the generators of quantum dynamical semigroups. Commun. Math. Phys. **48**(2), 119–130 (1976)
40. Kuhr, S., Gleyzes, S., Guerlin, C., Bernu, J., Hoff, U.B., Deléglise, S., Osnaghi, S., Brune, M., Raimond, J.M., Haroche, S., Jacques, E., Bosland, P., Visentin, B.: Ultrahigh finesse Fabry–Pérot superconducting resonator. Appl. Phys. Lett. **90**, 164101 (2007)
41. Dalibard, J., Castin, Y., Mølmer, K.: Wave-function approach to dissipative processes in quantum optics. Phys. Rev. Lett. **68**(5), 580–583 (1992)
42. Kollár, A.J., Papageorge, A.T., Vaidya, V.D., Guo, Y., Keeling, J., Lev, B.L.: Supermode-density-wave-polariton condensation with a Bose–Einstein condensate in a multimode cavity. Nat. Commun. **8**(14386), 17 (2017)
43. Hamsen, C., Tolazzi, K.N., Wilk, T., Rempe, G.: Strong coupling between photons of two light fields mediated by one atom. Nat. Phys. **14**, 885–889 (2018)